1971

A measurement of the capture coefficient and of the vapor pressure of CO_2 from 69°K to 80°K

Michel Louis Chouarain

A MEASUREMENT OF THE CAPTURE COEFFICIENT AND OF THE VAPOR PRESSURE OF CO_2 FROM 69°K TO 80°K

by

Michel Louis Chouarain, 1946-

A thesis

Submitted to the Faculty of

THE UNIVERSITY OF MISSOURI - ROLLA

In Partial Fulfillment of the Requirements for the

Degree of

MASTER OF SCIENCE IN CHEMISTRY

Rolla, Missouri

1971

Approved by

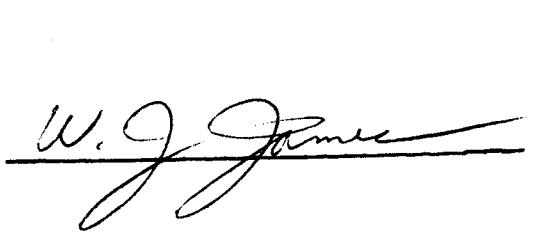

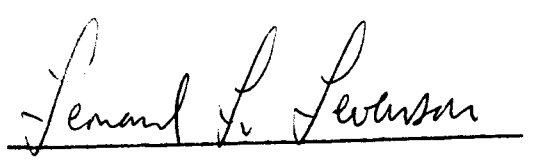

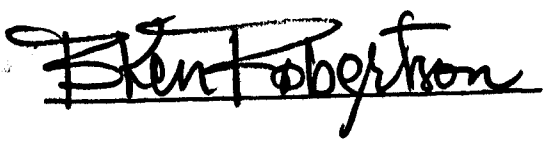

ABSTRACT

The capture coefficient of CO_2 gas at 135°K on a surface of CO_2 at temperatures between 69°K and 80°K is measured by means of quartz crystal microbalances. The vapor pressure of CO_2 is measured in the same range of temperature.

ACKNOWLEDGEMENTS

The author wishes to express his appreciation to Dr. L. L. Levenson, Assistant Professor of Physics and Senior Investigator at the Space Sciences Research Center, for suggesting the problem. His help and guidance are gratefully appreciated.

He would like to thank Dr. W. J. James, Professor of Chemistry and Director of the Graduate Center for Materials Research, for his continuous assistance and counsel.

The collaboration, interest and help from Mr. C. Bryson and V. Cazcarra all along in this investigation are gratefully appreciated.

A Research Assistantship from the Graduate Center for Cloud Physics Research is also gratefully acknowledged.

TABLE OF CONTENTS

LIST OF FIGURES

LIST OF TABLES

NOMENCLATURE

CB	:	Calorimeter copper block
CR	:	Calorimeter reflection microbalance
BM	:	Beam monitor microbalance
BMR	:	Beam monitor reflection microbalance
f_1	:	Frequency of the CR quartz crystal microbalance
f_2	:	Frequency of the BM quartz crystal microbalance
f_3	:	Frequency of the BMR quartz crystal microbalance
F	:	Geometrical factor between the source and BM
F'	:	Geometrical factor between the CB and CR
F_i	:	Geometrical factor between the source and area A_i of CB
F'_i	:	Geometrical factor between the area A_i of CB and CR
n_o	:	Flux emitted from the source
n'_o	:	Flux emitted from CB
γ	:	Capture coefficient
M	:	Molar mass of CO_2
P	:	Directly calculated vapor pressure
P_c	:	Vapor pressure corrected for the drift of the CR crystal
T_G	:	Molecular beam temperature
T_s	:	Calorimeter block temperature

I. INTRODUCTION

The capture coefficient γ of CO_2 on condensed CO_2 has been reported previously for different beam and surface temperatures and different beam intensities. Several authors[9-11] have given γ as ranging from 0.5 to 0.85 on surfaces at 77°K. Others[7,8] find $\gamma > 0.95$ at this surface temperature. It is important to resolve this discrepancy. A new apparatus built for this purpose is described here and experimental results are presented. In this work, γ is measured for a constant temperature of the beam (135°K) and a constant beam intensity (2.5×10^{13} molecules/s.cm^2). The use of quartz crystal microbalances improves greatly the sensitivity of the measurement. The method used is very direct, the only assumption being made that the emitting surfaces obey the cosine law.

II. PRINCIPLE OF THE MEASUREMENTS

The capture coefficient γ of a gas at a temperature T_G on a surface at a temperature T_s is defined as the ratio of the number of particles condensing on the surface to the number of incident particles.

The capture coefficient of CO_2 is measured between the temperatures of 69°K and 80°K using quartz crystal microbalances as particle detectors (Figures 1 and 8).

The microbalances are AT-cut quartz crystals[1,2] 15 mm in diameter and 0.34 mm thick. Evaporated gold electrodes, 6 mm in diameter, cover the central section (Figure 6) of these crystals. A transistorized electronic oscillator attached to the crystals holds them at their resonance frequency which is about 5 MHZ. The crystals are kept at constant temperature. A change of mass on the oscillating section (defined by the gold electrodes) causes a change of the resonance frequency. The frequency change is directly proportional to the mass change per unit area on the microbalance surface. The frequency measured by a frequency meter is made proportional to an electric potential. This potential is generated by a digital to analog converter and recorded as a function of time by a strip chart potentiometer. In this way, a change of mass versus time is continuously recorded.

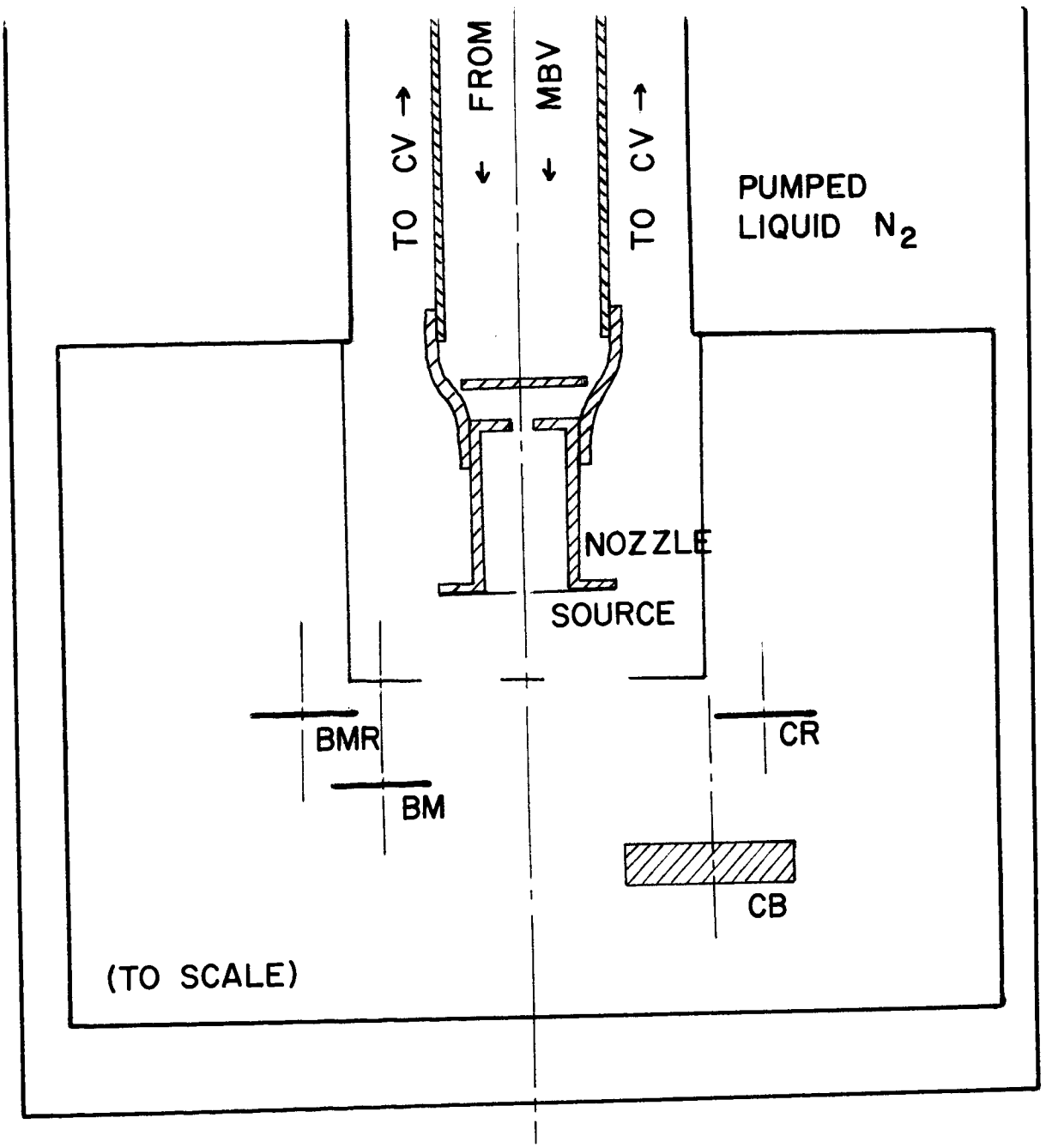

Figure 1. Molecular Beam Chamber.

The microbalances remain at a temperature (55°K) sufficiently low to make the capture coefficient very close to unity. A molecular beam of CO_2 is directed onto a beam monitor microbalance and a copper calorimeter block which is at the temperature T_s. The beam monitor microbalance permits the calculation of the flux intensity.

The gas reaching the calorimeter block is partly condensed. Those molecules not condensed on the block are reemitted and detected by a second microbalance located above the block (calorimeter reflection). A correction, evaluated when the beam is off, allows one to take into account the flux due to the sublimation of the gas on the calorimeter block. This last flux enables one to calculate the vapor pressure[3] of the gas at the temperature T_s. The flux at the center of a microbalance is given by the relationship

$$\text{Flux} = K \frac{df}{dt} \quad , \tag{1}$$

$\frac{df}{dt}$ being the rate of change of the frequency of the crystal versus time.

III. EXPERIMENTAL APPARATUS

A. Description

The molecular beam chamber is a cylinder containing mainly a copper block (main target), a target crystal (BM), two beam reflection crystals (BMR above the BM and CR above the copper block) and the molecular beam nozzle (Figures 1, 5, 6, 7). The chamber is maintained at an estimated base pressure of 10^{-9} torr by a liquid nitrogen-trapped oil diffusion pump and a surrounding of pumped liquid nitrogen. The molecular beam itself is controlled by an automatic pressure control valve which transfers gas from a reservoir into a reference volume maintained at a low pressure by another liquid nitrogen-trapped oil diffusion pump. The reference volume connects with the molecular beam chamber through a gas manifold (going through the molecular beam valve MBV), then through a tube 78.74 cm long ending in a nozzle (Figures 2, 3, 4); the beam passing through a 0.108 cm diameter hole in a tantalum foil. The opening and closing of the automatic pressure control valve creates or suppresses the beam.

The copper block is a disk of 2.54 cm diameter and a thickness of 0.615 cm. The two nylon screws on which it is mounted constitute the heat leak. Embedded in it are carbon, tin oxide and calibrated germanium resistors used to heat the block, maintain a constant temperature and

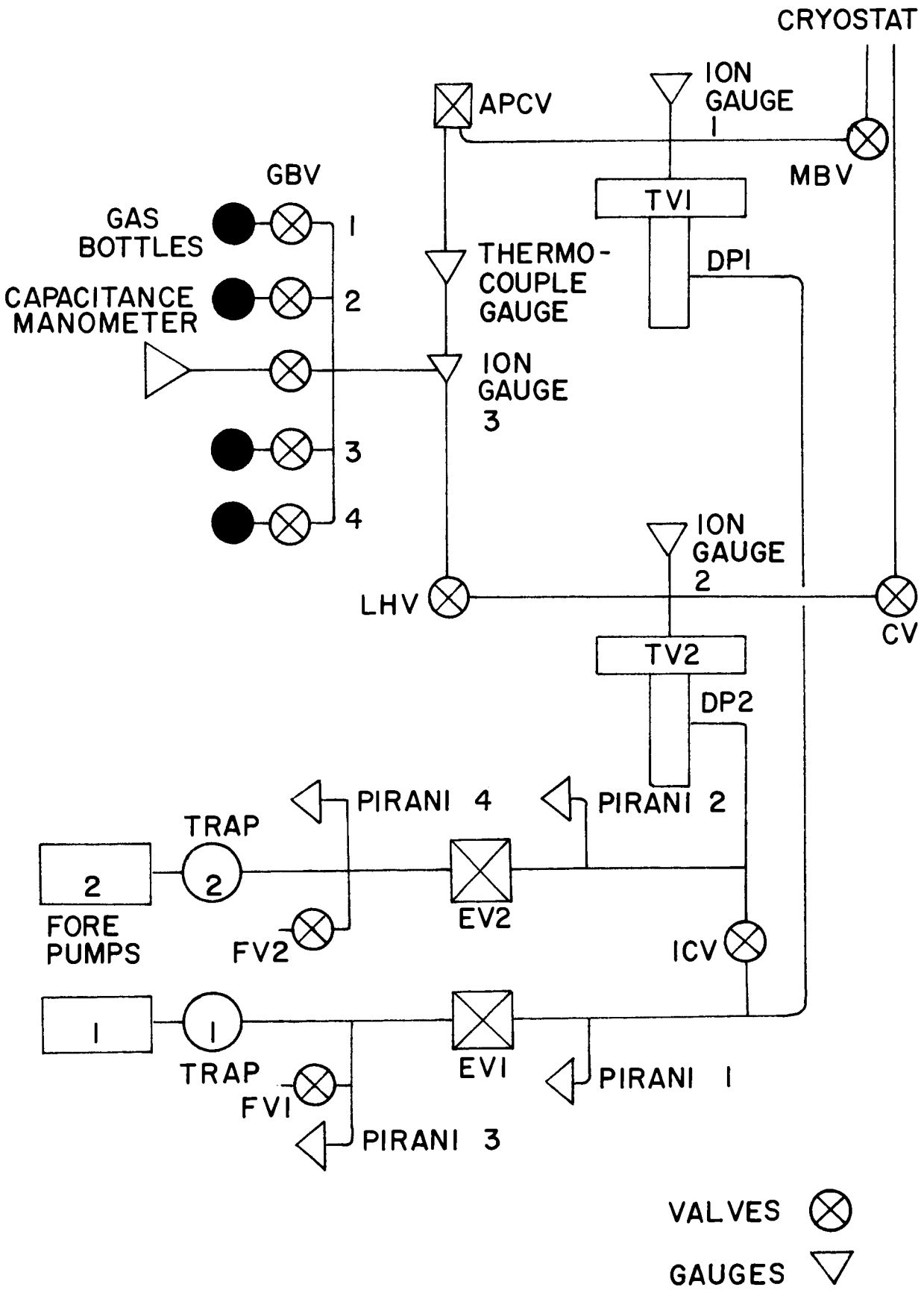

Figure 2. Vacuum System

Figure 3. Nozzle (Mounted)

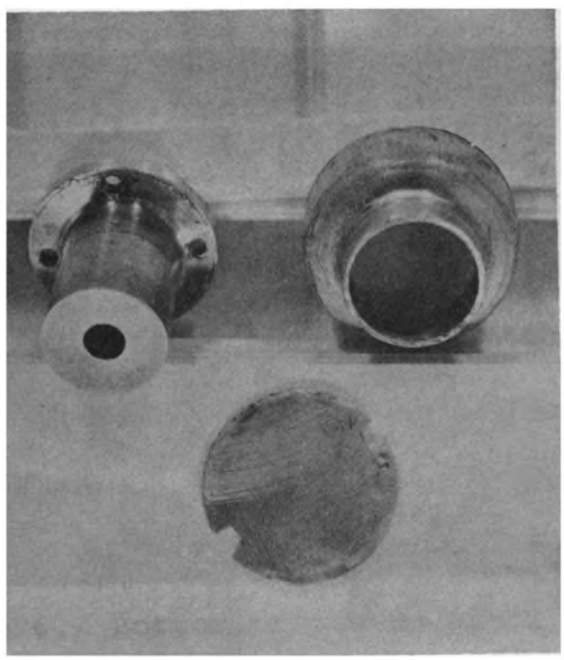

Figure 4. Nozzle (Unmounted)

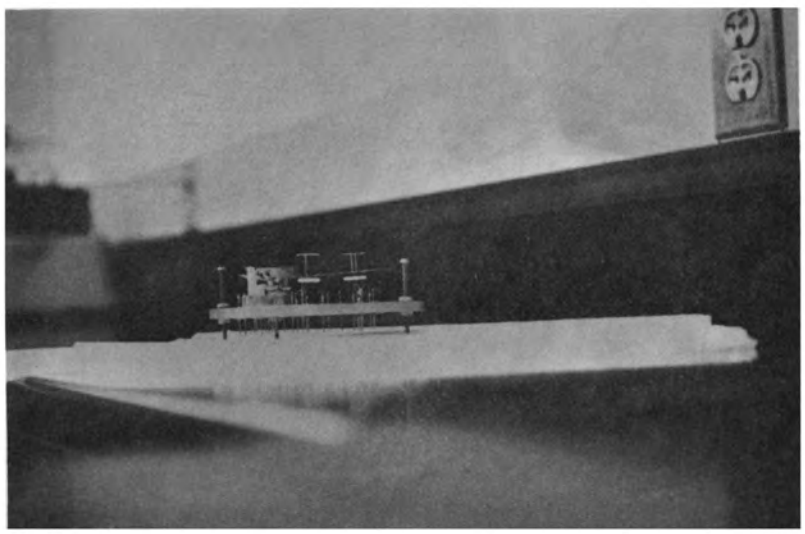

Figure 5. Bottom of the Molecular Beam Chamber (Side View)

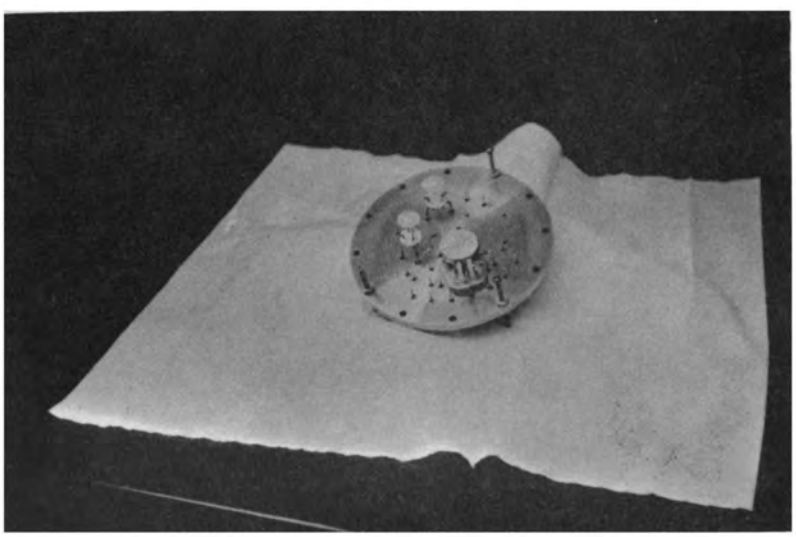

Figure 6. Bottom of the Molecular Beam Chamber

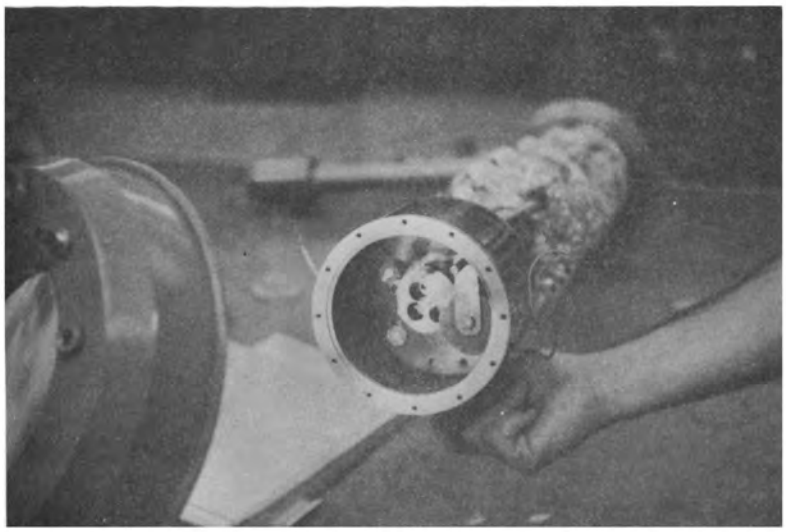

Figure 7. Top of the Molecular Beam Chamber

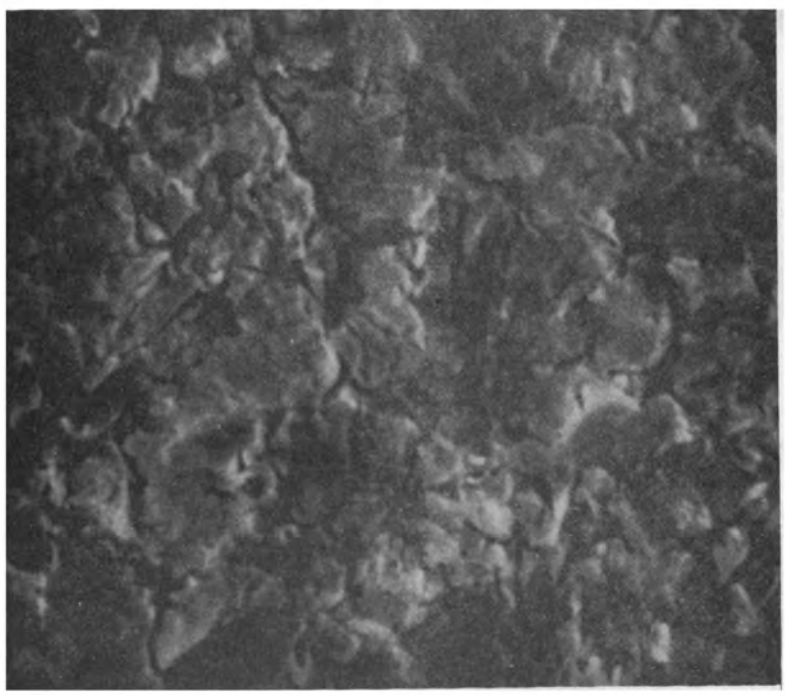

Figure 8. Surface of a Quartz Crystal Microbalance (X3000)

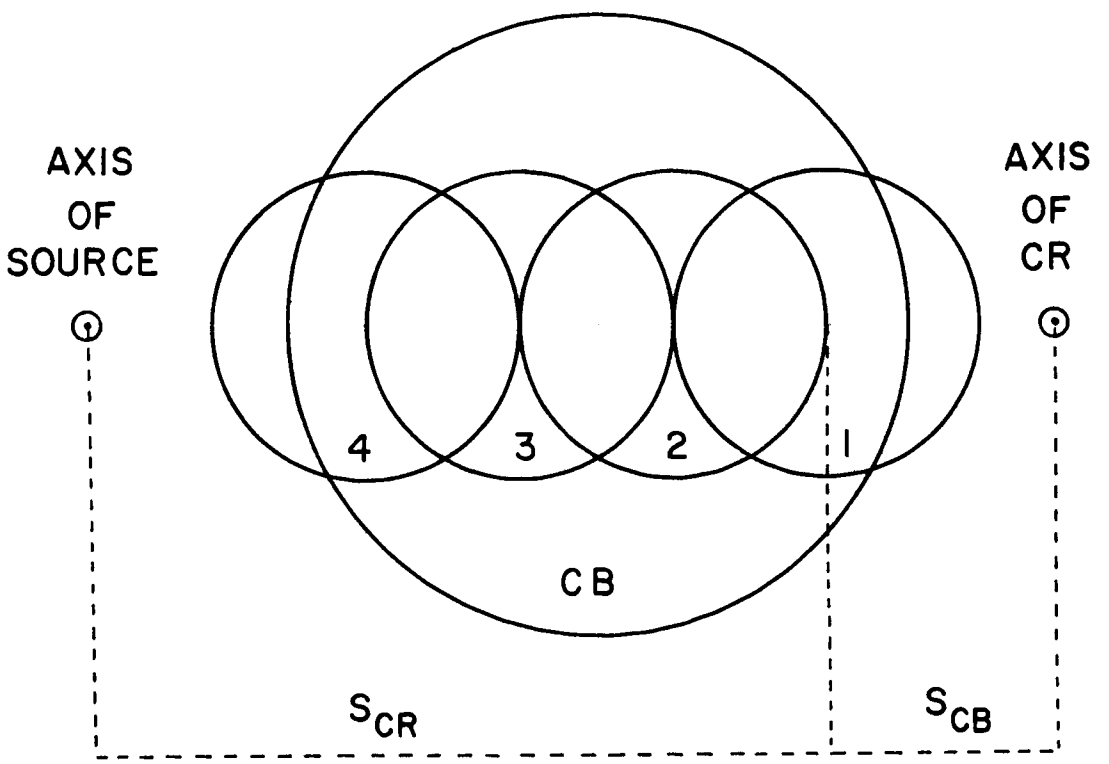

Figure 9. Approximation of the Geometrical Factor $\Sigma F_i F_i'$

measure that temperature. One of the wires of the germanium resistor is cemented to the block itself, creating a good thermal contact. All three resistors are cemented in place with GE 7031 low temperature varnish.

A germanium resistor is mounted on the nozzle to measure the temperature of the incoming beam. The temperature of the beam is made homogeneous by the structure of the nozzle.

The purity of the beam is at least 99.9% (value obtained from mass spectrometric data).

The molecular beam system (Figure 2) is fed by a group of gas bottles. The gas is admitted into a gas reservoir through the gas bottle valves GBV. The reservoir is bounded by the Log Roughing Valves (LRV), the Log High Vacuum Valve (LHV) and the Automatic Pressure Control Valve (APCV). The CO_2 is admitted through the APCV valve into a reference volume limited by the Trap Valve TV1 and the Molecular Beam Valve (MBV). The gas reservoir is kept at low pressure by Diffusion Pump 1 (DP1) via TV1. The gas goes to the molecular beam source through the MBV. The beam chamber (Figure 1) is kept under vacuum through the Diffusion Pump 2 (DP2), Trap Valve 2 (TV2) and the Chamber Valve (CV). The nomenclature of components shown in Figure 2 is summarized below:

Diffusion Pumps - DP 1, 2

Trap Valves - TV 1, 2

Top Manifold Valves

APCV	Automatic Pressure Control
LHV	Log High Vacuum
CV	Chamber Valve
MBV	Molecular Beam Valve

Gas Log Valves GBV (1 → 4) gas bottle valves

Foreline Valves

EV 1, 2	Electric Valves
FV 1, 2	Foreline Valves
ICV	Interconnection Valve

B. Geometrical Factors

The geometrical factors are calculated according to a procedure used by V.I. Lozgachev,[4] assuming that the spatial distribution of gas emission from each source obeys the cosine law.

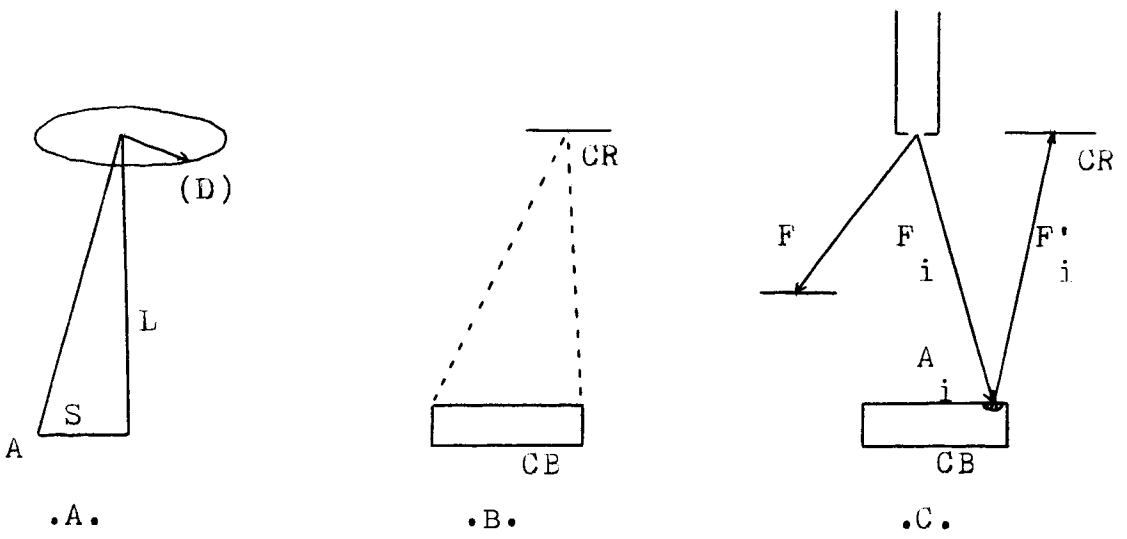

Figure 10. Geometry Used for Calculating the F Factors

The sources are circular, flat surfaces in all cases.

Consider Figure 10-A. If $\dot{N}_o$ is the flux (molecules/cm^2.s) from an emitting disc (D), the flux $\dot{N}_A$ at point A is calculated according to the following relationship:[4]

$$F = \frac{\dot{N}_A}{\dot{N}_o} = \frac{1}{2}\left[1 - \frac{L^2-R^2+S^2}{\sqrt{(L^2+R^2+S^2)^2 - 4R^2S^2}}\right] \qquad (2)$$

where F is called the geometrical factor, and L, R, and S are defined by Figure 10-A.

In this experiment, to measure the condensation coefficient, we determine the fraction of molecules reflected from the calorimeter block (CB). This fraction is

TABLE I

GEOMETRICAL FACTORS CALCULATIONS FOR THE BM, CB, CR

	L(cm)	R(cm)	S(cm)	F
BM	2.761	0.108	0.232	$0.526 \times 10^{-3} \pm 2 \times 10^{-6}$
CB	3.789	0.108	2.616	$0.372 \times 10^{-3} \pm 15 \times 10^{-6}$
CR	1.961	1.27	0.838	0.246 ± 0.002

TABLE II

GRADIENT OF FLUX ON THE CALORIMETER

S_{CB} (cm)	1.277	1.664	1.913	2.298	2.616	2.934	3.183	3.569	3.817
$F_i \times 10^3$	0.6539	0.57017	0.51528	0.63358	0.37214	0.31726	0.27906	0.22797	0.1992

TABLE III

CALCULATION OF THE GEOMETRICAL FACTOR $\Sigma F_i F'_i$

Area No. Fig. 9	S_{GB} (cm)	F_i	S_{CA} (cm)	F'_i	$F_i F'_i$
1	1.664	0.570×10^{-3}	0.705	0.032	0.182×10^{-4}
2	2.298	0.433×10^{-3}	0.455	0.057	0.247×10^{-4}
3	2.934	0.317×10^{-3}	0.205	0.085	0.269×10^{-4}
4	3.569	0.227×10^{-3}	0.045	0.094	0.216×10^{-4}

L = 3.789 cm

R = 0.108 cm

$\Sigma F_i F'_i = 0.913 \times 10^{-4}$

determined by the calorimeter reflection microbalance (CR). The fraction of molecules passing through the molecular beam orifice which reaches the surface of CB is $\sum_i F_i$, where F_i is the geometrical factor between the beam orifice and area A_i on CB. F'_i is the fraction of molecules reflected by area A_i (Fig. 10-C) on CB reaching CR. The fraction of molecules from the beam reaching CR is therefore, $\sum_i F_i F'_i$ if no condensation takes place. In the presence of condensation, this fraction is $(1 - \gamma) \sum_i F_i F'_i$.

If $\dot{n}_o$ is the total flux at the molecular beam orifice, and $\dot{n}'_o$ is the flux at CR, then

$$\frac{\dot{n}'_o}{\dot{n}_o} = (1 - \gamma) \Sigma F_i F'_i \qquad (3)$$

We determine n'_o by measuring the rate of frequency change of the quartz crystal CR. $\dot{n}_o$ is found from the rate of frequency change of the beam monitor crystal BM and the known geometrical factor F (Figure 10-C). To determine γ, it is only necessary to know the fixed geometrical factor $\sum_i F_i F'_i$. This quantity is approximated by dividing the block into four parts as shown in Figure 9. Each elementary disc has an area of one-fourth the total area. These calculations yield $\sum_i F_i F'_i = 0.913 \times 10^{-4} \pm 5 \times 10^{-7}$ (Tables I, II).

We determine the flux of sublimation by considering that the block itself is emitting homogeneously from all

over its surface.(Fig. 10-B). This flux is detected by CR. The geometrical factor F' corresponding to this situation is according to equation (2):

$$F' = 0.246 \pm 0.002 \qquad \text{(Table I)}$$

We can compare $\sum_i F_i F'_i$ to the product of the geometrical factor between the beam and the center of the calorimeter block by F'. This product is 0.9155×10^{-4}.

These values do not differ much since the CR crystal microbalance is opposite to the source across the calorimeter, and the distances on each A_i compensate each other.

C. Procedure

As previously stated, the flux at the center of a microbalance is proportional to the rate of change of its frequency.

The intensity of the molecular beam, recorded by means of the BM, is the same for all the measurements (2.5×10^{13} molecules/s.cm^2). When the beam is off, the variation of frequency of the BM is equal to zero. When the beam is on, a slope corresponding to the variation of frequency, is recorded on the strip chart. This slope is the same for all the measurements (Figure 11).

The measurements are made with the CR crystal. At the beginning of each run, the temperature of the block is the temperature of the surrounding, pumped liquid nitrogen (55-57°K). The drift slope of this crystal is

then recorded and several hundred layers of gas are condensed on the calorimeter block.

The block is then heated to the temperature T_s. A frequency versus time base line is recorded for the CR crystal. The beam is then turned on, creating a new slope. The beam is then turned off, and a new base line (which should be parallel to the first one recorded) is obtained.

The block is then heated to a different temperature and the operation is resumed (Figure 11). The temperature, T_s, is recorded several times during each operation.

A residual power must be left in the heating resistor in order to maintain the temperature T_s at a constant value.

D. Calculations

If $\dot{n}_o$ is the flux emitted from the molecular beam source, the flux reaching the beam monitor (BM) is

$$F\dot{n}_o \qquad \text{(molecules/cm}^2\text{.s)} \qquad (4)$$

The variation of frequency on the BM is

$$\left(\frac{df_2}{dt}\right)_{on} = KF\dot{n}_o = S \qquad \text{(Hz/s)} \qquad (5)$$

The flux reaching the area A_i of the copper block is

$$F_i\dot{n}_o \qquad (6)$$

The flux reaching the center of the CR coming from A_i is

$$(1 - \gamma)\, \dot{n}_o \Sigma_i F_i F'_i \tag{7}$$

The total flux reaching the center of the CR is

$$F'\dot{n}'_o + (1 - \gamma)\dot{n}_o \Sigma_i F_i F'_i = \frac{1}{K} \left(\frac{df_1}{dt}\right)_{on} \tag{8}$$

where $\dot{n}'_o$ is the flux sublimating from the surface of CB. To determine $\dot{n}'_o$ the beam is turned off. Then,

$$KFn'_o = \frac{df_1}{dt} \tag{9}$$

where $\frac{df_1}{dt}$ is the rate of change of frequency of CR.

If we define,

$$s = \left(\frac{df_1}{dt}\right)_{on} - \left(\frac{df_1}{dt}\right)_{off}, \tag{10}$$

we have the following relationship:

$$\frac{s}{S} = (1 - \gamma) \frac{\Sigma_i F_i F'_i}{F} \tag{11}$$

It should be noted that equation (11) shows that the determination of γ does not depend on the proportionality constant K which appears in equations (1), (5), (8) and (9).

The flux reaching the center of a crystal microbalance is known from the variation of frequency of this crystal:

$$\dot{n} = -\frac{1.079\ 10^{16}}{M}\ \frac{df}{dt} = K\ \frac{df}{dt}(\text{molecules}/\ \text{cm}^2).$$

(12)

The slopes (linear rate of change of frequency) are measured by the quantities N and D defined in Figure 11. They are recorded on a strip chart 25 cm wide, with a chart speed v and a sensitivity σ (number of Hertz full scale).

If N is in cm

D is in cm

v is in cm/mn (Figure 11),

the value of a slope in Hertz/s is

$$\frac{df}{dt} = \frac{1}{25} \times \frac{1}{60}\ \sigma v\ \frac{N}{D} \qquad (13)$$

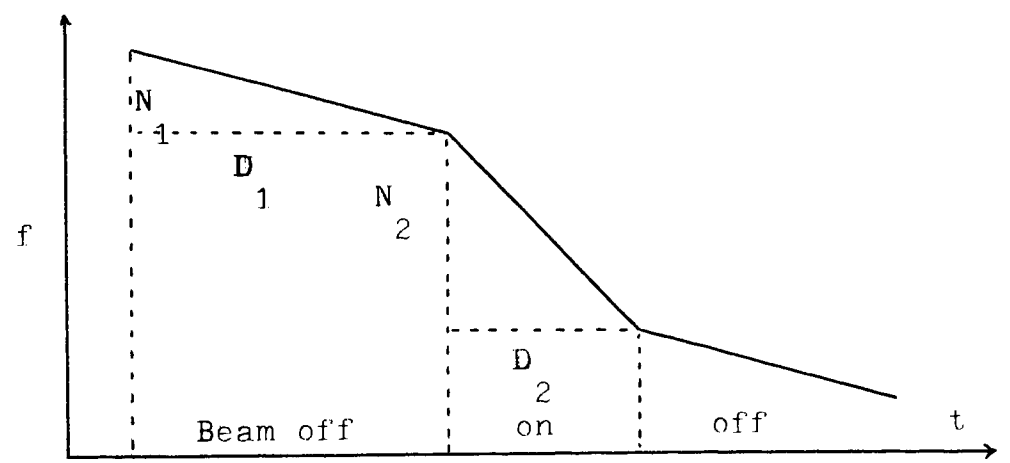

Figure 11. Frequency Histogram

One obtains:

$$(1 - \gamma) = \left(\frac{N_2}{D_2} - \frac{N_1}{D_1}\right) \frac{\sigma v}{\sigma_3 v_3} \frac{D_3}{N_3} \frac{F}{\Sigma F_i F_i'} \qquad (14)$$

where subscript 3 refers to quantities recorded with the beam monitor crystal (BM), i.e., related to the molecular beam intensity.

The vapor pressure is related to the flux of subliming gas at the surface of the calorimeter block at the temperature T_s by:

$$\dot{n} = \frac{\gamma P_s}{\sqrt{2 \pi m k_B T_s}} \qquad (15)$$

$\dot{n}$ corresponds to S_1 when the beam is off. From equations 2 and 10,

$$|\dot{n}| = \frac{1}{F'} \frac{1.079\ 10^{16}}{M} \left(\frac{df_1}{dt}\right)_c \qquad (16)$$

P (in Torr) is expressed by the following relationship:

$$P = 0.308\ 10^{-10} \frac{\sigma v}{F'} \frac{N_1}{D_1} \frac{\sqrt{T}}{\gamma} \qquad (17)$$

P_c is the value of P corrected for the drift of the CR crystal, assuming that this drift remains constant during each experiment. We define P_4 drift pressure as

$$P_4 = 0.308 \times 10^{-10} \frac{\sigma_4 v_4}{F'} \frac{N_4}{D_4} \sqrt{T_4}$$

T_4, σ_4, v_4, N_4 and D_4 being the values corresponding to the drift when it is recorded at the beginning of each experiment. (γ is equal to 1 in these conditions). P_c is then equal to $P - P_4$.

In practice, the frequency of the CR crystal may drift at a constant rate because of a slow change of the cryostat wall temperature. This frequency drift, if any, is recorded before the condensation coefficient and vapor pressure experiments are carried out. When present, the drift rate is constant several hours before an experiment is performed. It is assumed, therefore, that this drift is constant during the interval in which experimental data are taken. However, it is necessary to take account of the frequency drift only during the first hour or two of the experiment, when T_s is below 68°K and the sublimation rate from the copper block is too small to measure. When $T_s \geq 69$°K, the rate of frequency change due to sublimation is a decade larger than the drift rate.

IV. DATA AND RESULTS

The data and results are displayed respectively in Tables IV, V, VI, and VII, VIII, IX.

Each data point includes:

the initial drift of the CR, N_4, D_4, σ_4, v_4 ,

the slope corresponding to the beam monitor, N_3, D_3, σ_3, v_3 ,

the temperature at which each manipulation is done, and

the values of N and D with the beam off (N_1,D_1) and the beam on (N_2, D_2), the chart speed v and sensitivity (Figure 11)

These sets of data are tabulated, corresponding to different runs.

The slope corresponding to the beam monitor (N_3, D_3, σ_3, v_3) is the same for all the values (constant flux).

$N_3 = 1.5$, $D_3 = 17.2$, $\sigma_3 v_3 = 2500$.

The results are obtained according to the previous section. They were computed on a Wang 700 calculator. Tables VII, VIII, and IX yield the values of γ, capture coefficient, $\Delta\gamma$, error on γ (see Appendix A), Pc, corrected pressure and ΔPc error on Pc (see Appendix A).

TABLE IV

SET OF DATA

NUMBER 1

N°	T(°K)	N_1 (cm)	D_1 (cm)	N_2 (cm)	D_2 (cm)	σv (Hz·cm/mn)
1	69.7	6.1	20	9.9	20	0.5
2	71.6	6.9	10	9.8	10	0.5
3	74.0	14.7	7	18.8	6.1	0.5
4	76.2	14.6	12.3	17.2	10.7	2.5
5	78.6	14.5	20	18.2	20	15

Drift = N_4 = 3.5 cm, D_4 = 20 cm, $\sigma_4 v_4$ =0.5 Hz·cm/mn

T_4 = 59°K

TABLE V

SET OF DATA

NUMBER 2

N^{o}	T(°K)	N_1 (cm)	D_1 (cm)	N_2 (cm)	D_2 (cm)	σv (Hz·cm/mn)
1	71.8	9.4	4.7	13.4	5.2	0.5
2	71.6	7.1	19.3	8.6	17.5	2.5
3	75.3	17.1	16.5	17.7	13.2	2.5
4	74.9	11	10.7	15.3	11.7	2.5
5	77.2	12.4	10	14.9	9.9	5
6	77.0	17.1	12.3	16.8	10.8	5
7	77.0	16.8	12.3	14.7	8.4	5
8	77.9	16.3	12.3	20	12.8	5
9	79.0	18.1	6	*	*	5
10	81.1	10.9	6.7	*	*	25

Drift: $N_4 = 10.3$, $D_4 = 9.9$, $\sigma_4 v_4 = 0.5$ $T_4 = 57°K$

*Note: The values of N_2 and D_2 do not differ from N_1 and D_1 with the incertitude on the reading. No value of γ can be obtained from these measurements.

TABLE VI

SET OF DATA

NUMBER 3

N°	T°K)	N_1 (cm)	D_1 (cm)	N_2 (cm)	D_2 (cm)	σv (Hz·cm/mn)
1	76.7	6.5	20.7	9.1	21.9	12.5
2	75.9	5.3	17.1	9.1	21.9	12.5
3	77.3	8.9	20	10.1	18	12.5
4	79.3	13.1	8.35	9.95	5.5	12.5
5	79.4	11.2	6.8	9.95	5.5	12.5
6	74.1	2.2	9	6.5	17.8	5
7	79.3	4.0	18.1	5.3	16	5
8	76.9	9.5	14	9.1	9.8	5
9	76.9	7.5	11.2	9.1	9.8	5
10	76.9	6.2	18.6	8.0	18.8	12.5
11	76.9	5	16.2	8.0	18.8	12.5

Drift: $N_4 = 2.6$, $D_4 = 27$, $\sigma_4 v_4 = 5$ $T_4 = 55°K$

TABLE VII

SET OF RESULTS

NUMBER 1

N°	$\frac{1000}{T}(°K^{-1})$	γ	$\Delta\gamma$	Pc(Torr)	ΔPc(Torr)
1	14.35	0.9975	7×10^{-4}	6.81×10^{-11}	3.6×10^{-12}
2	13.97	0.9962	9×10^{-4}	2.74×10^{-10}	1.6×10^{-11}
3	13.51	0.987	5×10^{-3}	1.05×10^{-9}	6×10^{-11}
4	13.11	0.972	7×10^{-3}	3.24×10^{-9}	1.5×10^{-10}
5	12.72	0.93	2×10^{-2}	1.29×10^{-8}	6×10^{-10}

TABLE VIII

SET OF RESULTS

NUMBER 2

N°	1000/T	γ	Δγ	Pc(Torr)	ΔPc(Torr)
1	13.92	0.9924	3.3×10^{-3}	5.13×10^{-10}	3.9×10^{-11}
2	13.96	0.9918	1.6×10^{-3}	4.26×10^{-10}	2.1×10^{-11}
3	13.27	0.9799	4.5×10^{-3}	2.79×10^{-9}	9×10^{-11}
4	13.35	0.9815	4.4×10^{-3}	2.26×10^{-9}	1.1×10^{-10}
5	12.95	0.965	9×10^{-3}	6.47×10^{-9}	3.5×10^{-10}
6	12.98	0.9782	5.4×10^{-3}	7.22×10^{-9}	3.1×10^{-10}
7	12.98	0.969	1.3×10^{-2}	7.30×10^{-9}	3.8×10^{-10}
8	13.01	0.9686	7.5×10^{-3}	6.92×10^{-9}	3.2×10^{-10}
9	12.65	*	*	1.65×10^{-8}	1.0×10^{-9}
10	12.33	*	*	4.57×10^{-8}	2.8×10^{-9}

*Cf. Table V.

TABLE IX

SET OF RESULTS

NUMBER 3

N°	1000/T	γ	$\Delta\gamma$	Pc(Torr)	ΔPc(Torr)
1	13.03	0.9655	6.3×10^{-3}	3.91×10^{-9}	2.2×10^{-10}
2	13.17	0.9651	6.6×10^{-3}	3.83×10^{-9}	2.5×10^{-10}
3	12.93	0.9616	7.4×10^{-3}	5.82×10^{-9}	2.9×10^{-10}
4	12.60	0.921	2.6×10^{-2}	2.32×10^{-8}	1.8×10^{-9}
5	12.60	0.947	1.8×10^{-2}	2.37×10^{-8}	1.8×10^{-9}
6	13.49	0.9840	3.3×10^{-3}	8×10^{-10}	1×10^{-10}
7	13.60	0.9854	2.8×10^{-3}	6.8×10^{-10}	5×10^{-11}
8	13.00	0.9669	7.4×10^{-3}	3.30×10^{-9}	1.7×10^{-10}
9	13.00	0.9658	7.9×10^{-3}	3.26×10^{-9}	2.0×10^{-10}
10	13.00	0.9695	5.8×10^{-3}	4.17×10^{-9}	2.4×10^{-10}
11	13.00	0.9614	7.5×10^{-3}	3.85×10^{-9}	2.7×10^{-10}

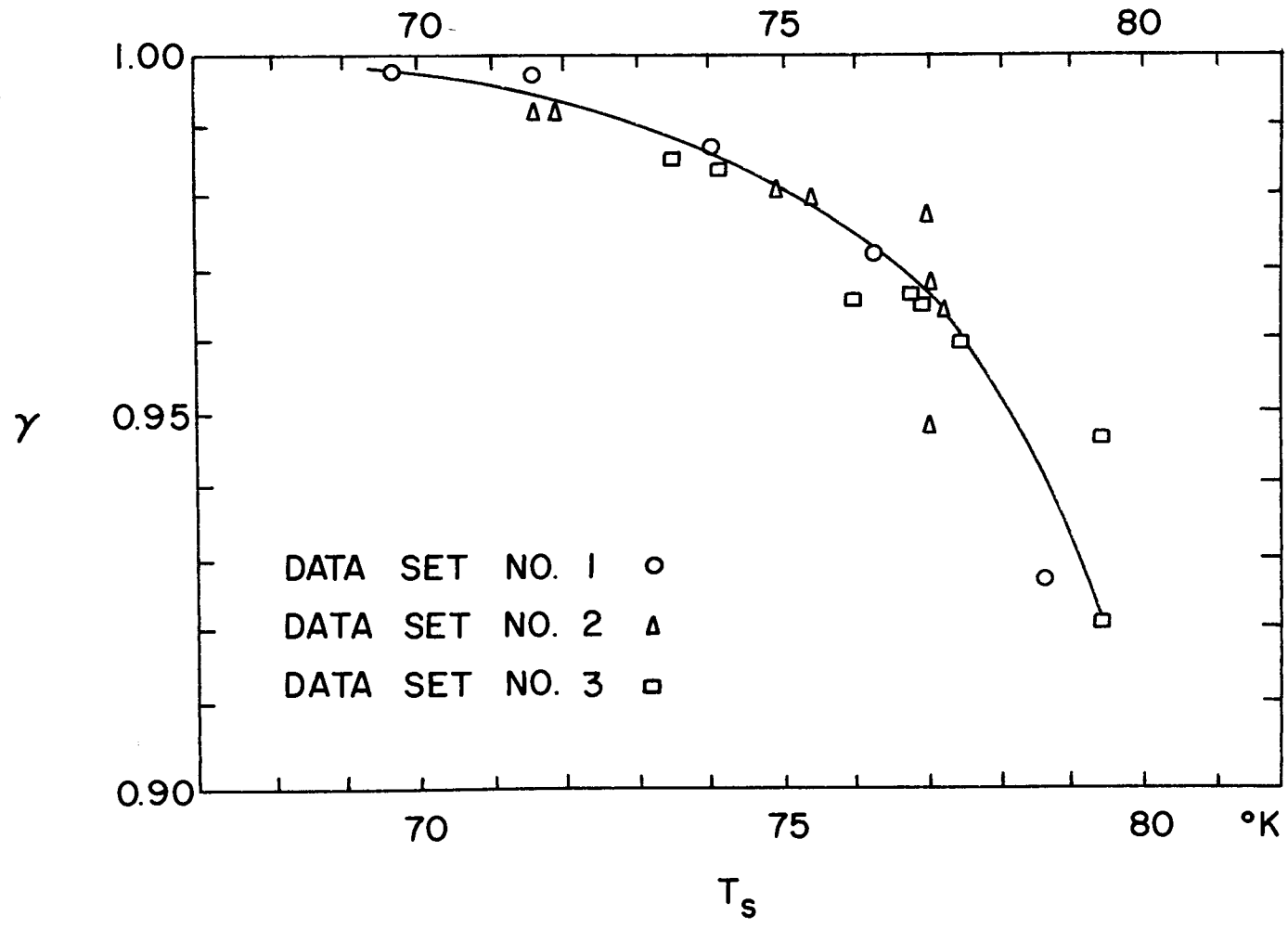

Figure 12. Capture Coefficient of CO_2 Versus Temperature

Figure 13. Vapor Pressure of CO_2 Versus Temperature

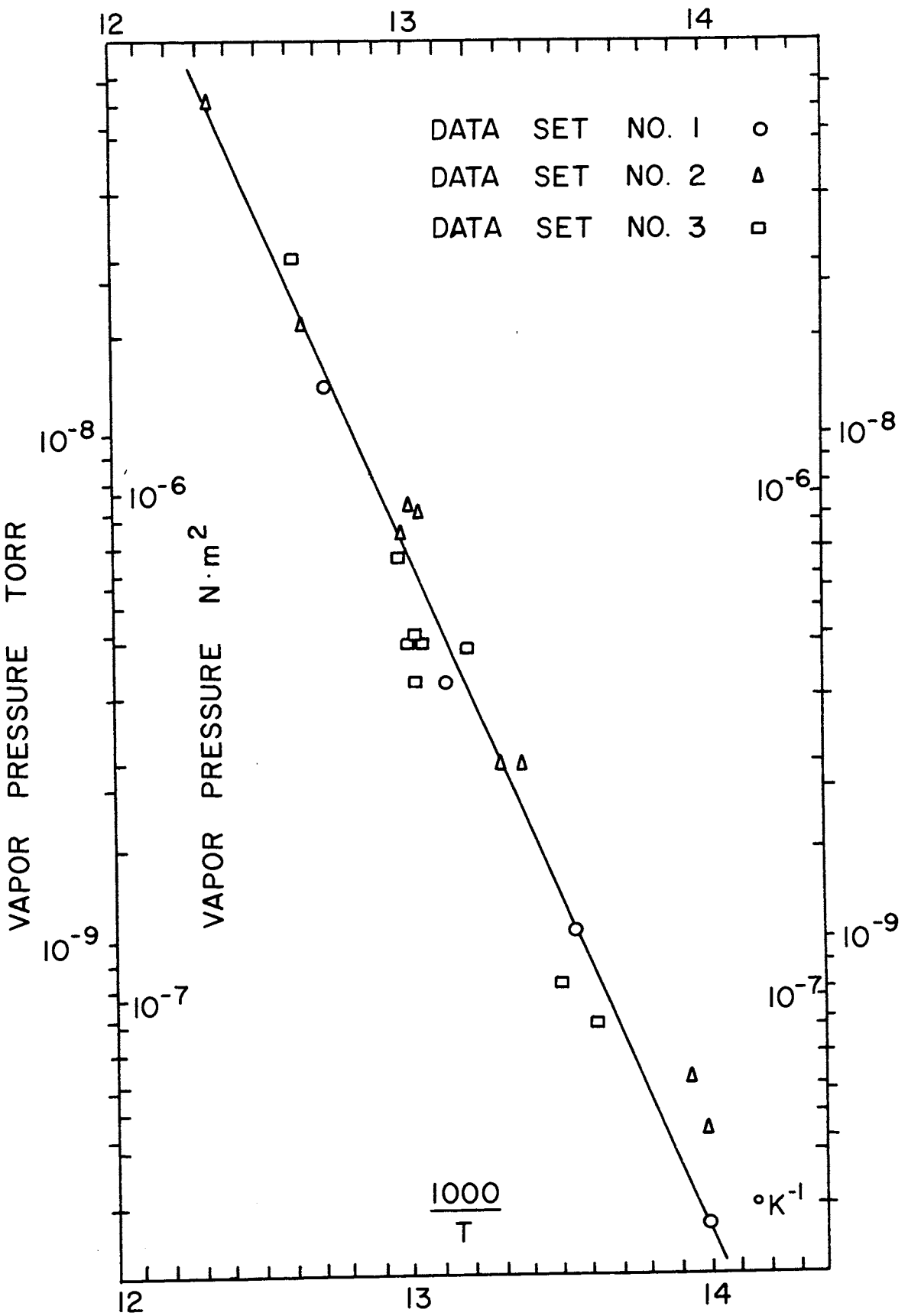
12
13
14
DATA SET NO. 1
DATA SET NO. 2
DATA SET NO. 3
10^{-8}
10^{-6}
10^{-9}
10^{-7}
VAPOR PRESSURE TORR
VAPOR PRESSURE N·m^2
$\frac{1000}{T}$
°K^{-1}

Figure 13

TABLE X

PREVIOUSLY PUBLISHED VALUES OF γ

Gas Temperature °K	Surface Temperature °K	Impingement Rate molecules/cm^2.s	γ	Reference
300	77	$<2 \times 10^{16}$	0.6	11
300	77	10^{15}	0.7	10
150 to 400	79	$<2 \times 10^{16}$	1.0	12
195	77	$<10^{16}$	0.85	9
300	74	2×10^{14}	1.0	7
300	77	2×10^{14}	0.95	7
300	77	2×10^{14}	0.85	7
400	77	10^{16}	0.49	0
195	10 to 20	10^{16}	>0.90	9
300	77	10^{16}	0.63	9
300	77	10^{16}	0.99	8

V. CONCLUSIONS

A method of measuring the capture coefficients γ of various gases has been described. This method has been applied to measure γ for CO_2. The gas temperature of 135°K was used for these experiments. For surface temperatures T_s between 60° and 69°K, $\gamma = 1.0000 \pm 5 \times 10^{-4}$. At higher values of T_s, γ decreases, with $\gamma = 0.92 \pm 2.6 \times 10^{-2}$ at $T_s = 79.3$°K.

The apparatus described is also capable of giving the sublimation rates of condensed gases. By assuming the sublimation coefficient α to be equal to the measured condensation coefficient γ, the equilibrium vapor pressure of a condensed gas can be calculated. For CO_2 it is found that the pressure-temperature relationship is

$$\ln P = \frac{3174.6}{T} + 22.263$$

with T in °K and P in Torr (cf. Appendix B).

The slope of the curve lnP versus 1/T yields the enthalpy change for sublimation, ΔH_s. This is found to be $\Delta H_s = 6308$ cal/mole $\pm$ 200 cal/mole. The vapor pressure of CO_2 determined here is about a factor of 3 lower than the extrapolated curve given by Honig and Hook.[13] However, ΔH_s corresponds well with the value found from the Honig and Hook extrapolation, $\Delta H_s = 6305$ cal/mole.

In the temperature range 55 to 68°K, γ was obtained by recording the CR crystal frequency as a function of time while condensing a known quantity of CO_2 on the calorimeter block. The CR crystal frequency did not change within the accuracy of our frequency measurement. This result could only be obtained if $\gamma = 1.0000 \pm 5 \times 10^{-4}$. The possible error indicated is due to the accuracy limitation of the frequency measurements ($\pm$0.001 Hz) during these experiments.

The main factors involved for the accuracy of the data obtained are the temperature and the geometrical factors. The temperature is measured with a calibrated germanium resistor thermometer. The errors on each temperature are less than 0.2K.

The errors introduced by the imprecision of determining the geometrical factors are derived in Appendix A. The relative probable errors of the condensation coefficient γ and of the vapor pressure P_c are taken to be equal to the sum of the relative errors of the measured and calculated quantities. Thus, the expected relative errors $\frac{\Delta\gamma}{\gamma}$ and $\frac{\Delta P}{P}$ always exceed the relative precision of the individual measurements made during an experiment.

Our data agree with similar values reported in the literature, if we take into account the differences due to the temperature and intensity of the beam (cf. Table X and ref. 7). The method used allows to improve greatly the

accuracy both on the measurements of the capture coefficient and of the vapor pressure. The difference found in our values of the vapor pressure and the values reported in ref. 13 is not surprising since Honig and Hook's extrapolation goes seven decades in pressure beyond the range of pressure covered by previous measurements.

VI. APPENDICES

APPENDIX A

Errors

From equations 17 and 14, the values of the pressure and of the condensation coefficient are given by the relationships

$$P = 0.308 \times 10^{-10} \frac{\sigma v}{F'} \frac{N_1}{D_1} \frac{\sqrt{T}}{\gamma} \tag{1}$$

$$(1 - \gamma) = \left(\frac{N_2}{D_2} - \frac{N_1}{D_1}\right) \frac{\sigma v}{\sigma_3 v_3} \frac{D_3}{N_3} \frac{F}{\Sigma F_i F'_i} \tag{2}$$

By differentiation of equation (1), supposing that there is no error on σ and v, and that γ is an independent variable, we get

$$\frac{dP}{P} = \frac{dF'}{F'} + \frac{dN_1}{N_1} + \frac{dD_1}{D_1} + \frac{dT}{2T} + \frac{d\gamma}{\gamma} \tag{3}$$

going to finite errors with $\Delta N_1 = \Delta D_1 = \Delta L$

$$\frac{\Delta P}{P} = \frac{\Delta F'}{F'} + \frac{\Delta \gamma}{\gamma} + \frac{\Delta T}{2T} + \Delta L \left(\frac{1}{N_1} + \frac{1}{D_1}\right) \tag{4}$$

If we define $s' = \frac{N_2}{D_2} - \frac{N_1}{D_1}$, differentiation of equation (2) yields

$$\frac{d(1-\gamma)}{1-\gamma} = \frac{d\gamma}{1-\gamma} = \frac{ds'}{s'} + \frac{dD_3}{D_3} + \frac{dN_3}{N_3} + \frac{dR}{R} \qquad (5)$$

From our definition of s'

$$s' = \frac{N_2D_1 - N_1D_2}{D_1D_2} \qquad (6)$$

and the differentiation of s' yields

$$ds' = dN_1 \left(\frac{-D_2}{D_1D_2}\right) + dN_2 \left(\frac{D_1}{D_1D_2}\right)$$

$$+ dD_1 \left[\frac{N_2D_1D_2 - (N_2D_1 - N_1D_2)D_2}{(D_1D_2)^2}\right]$$

$$+ dD_2 \left[\frac{-N_1D_1D_2 - (N_2D_1 - N_1D_2)D_1}{(D_1D_2)^2}\right] \qquad (7)$$

which gives

$$ds' = \frac{dN_1}{D_1} + \frac{dN_2}{D_2} + dD_1 \frac{N_1}{D_1^2} - dD_2 \frac{N_2}{D_2^2} \qquad (8)$$

going to finite errors, equations (5) and (7) yield

$$\frac{\Delta\gamma}{1-\gamma} + \frac{\Delta R}{R} + \Delta L \left[\frac{1}{(N_2D_1-N_1D_2)}(D_1+D_2+N_1\frac{D_2}{D_1} + N_2\frac{D_1}{D_2}) + \frac{1}{D_3} + \frac{1}{N_3}\right] \qquad (9)$$

with $\Delta L = \Delta D_1 = \Delta D_2 = \Delta D_3 = \Delta N_1$.

The error on N and D (L) is less than 0.2 cm. The errors calculated on the geometrical factors are respectively

$$\Delta F = 2 \times 10^{-6} \qquad \Delta(\Sigma_i F_i F_i') = 5 \times 10^{-7}$$

$$\Delta F' = 2 \times 10^{-3} \qquad \frac{dR}{R} = 0.01$$

The values of the temperatures are obtained by linear interpolation from the calibration data supplied with the commercial resistance thermometers.

The error on the condensation coefficient increases when the temperature T_s increases, because of the interference caused by the sublimation of CO_2.

On the other hand, the error on the vapor pressure measurements decreases when the temperature T_s increases. The precision on γ when $\gamma \to 1$ is limited by the sensitivity of the microbalances.

Figure 14 indicates the calculated value of the

error on γ as a function of γ.

The value of the ratio of the geometrical factors was checked by condensing a measured amount of CO_2 on the block and letting it evaporate completely. The ratios of the changes of frequencies on BM and BMR yield $\frac{F}{\Sigma F_i F_i'}$ The value recorded was 15% lower than the calculated value. However, the agreement is satisfactory because the second term in equation (9) given in this Appendix is always much larger than the first term, $\Delta R/R$ where $R = \frac{\Sigma_i F_i F_i'}{F}$.

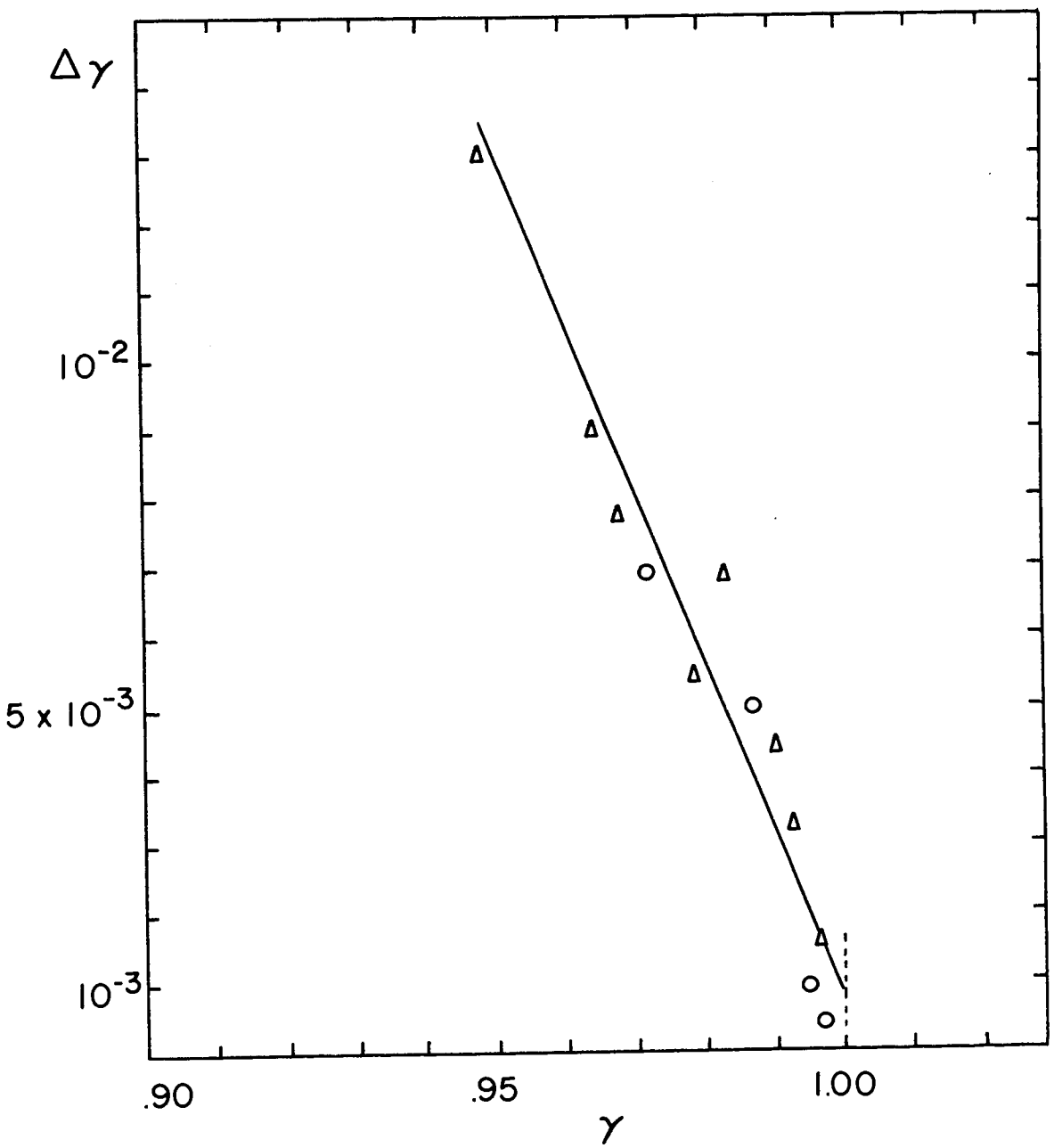

Figure 14. Probable Error on the Capture Coefficient

APPENDIX B

Relationship Between T and P

The least square method is used to compute the equation T + f(P) from data obtained in Tables VII, VIII and IX. We define

$$y_i = \frac{1000}{T}$$

$$x_i = \ln Pc$$

{ For each data point there are n data points available (n = 26).

We look for a relationship of the kind

$$y = ax + b$$

The values of a and b are computed from:

$$\bar{x} = \frac{\Sigma_i y_i}{n}$$

$$\bar{x} = \frac{\Sigma_i x_i}{n}$$

$$b = \frac{\Sigma_i (x_i - \bar{x}) y_i}{\Sigma_i (x_i - \bar{x})^2}$$

$$a = \bar{y} - b\,\bar{x}$$

The value of the enthalpy of sublimation ΔH is

$$\Delta H = E = \frac{1.99 \times 10^3}{a}$$

The probable errors on each quantity are

$$S_a = \left[\frac{1}{n} \frac{\Sigma_i (x_i-\bar{x})^2 (a_i-a)^2}{\Sigma_i (x_i-\bar{x})^2} \right]^{1/2}$$

$$S_b = \left[\frac{1}{n} \frac{\Sigma_i (x_i-\bar{x})^2 (b_i-b)^2}{\Sigma_i (x_i-\bar{x})^2} \right]^{1/2}$$

with

$$a_i = \frac{\bar{y}x_i - \bar{x}y_i}{x_i-\bar{x}}$$

$$b_i = \frac{y_i-\bar{y}}{x_i-\bar{x}}$$

The probable error on E is

$$S_E = S_b \cdot \frac{E}{b}$$

These values were computed on a Hewlett Packard 2000 calculator. They are:

$a = 7.013$ $\quad S_a = 0.213$

$b = -0.31480$ $\quad S_b = 1.09 \times 10^{-2}$

$E = 6321$ $\quad S_E = 200$

VII. BIBLIOGRAPHY

1. L.L. Levenson, Thesis, University of Paris (1968).

2. L.L. Levenson, "Condensation Coefficients of Argon, Krypton and Xenon Measured with a Quartz Crystal Microbalance at 4.2°K," Supplemento Al Nuevo Cimento 5, 321 (1967).

3. L.L. Levenson, CR Ac. Sciences, Paris 265 series B, 1217 (1967).

4. V.I. Lozgachef, Soviet Physics - Technical Physics 7, 736 (1963).

5. J.C. Mullins, B.S. Kirk and W.T. Ziegler, Tech. Rept. No. 2, Project No. A-663 (Engineering Experiment Station, Georgia Institute of Technology, August 1963).

6. L.O. Mullen and M.S. Hiza, J. Vac. Sci. and Tech. 4, 219 (1967).

7. R.F. Brown, D.M. Trayer and M.R. Busby, J. Vac. Sci. and Tech. 7, 241 (1970).

8. T.L. Moody, AEDC-TR-66-231, January 1967.

9. J.P. Dawson and J.D. Haygwood, Cryog. 5, 57 (1965).

10. G. Sanger, DLR FB 64-17, DLV-Bericht 320 (1964) Deutsche Versuchtstangstalt fur Luft-und-Raumfahrt, E.V., Institute fur Raumsimulation, Polz-Wahn, West Germany.

11. E.S.J. Wang, J.A. Collins, Jr., and J.D. Haygwood, Advances in Cryogenic Engineering 8, 73 (1963).

12. B.A. Buffham, P.B. Henault and R.A. Flinn, Vac. Symp. Trans. 9, 216 (1962).

13. R.E. Honig and H.O. Hook, RCA Review 21, 360 (1960).

14. R.F. Brown and E.S. Wang, Adv. Cryog. Eng. 10, 283 (1964).

15. J.H. Heald, Jr., and R.F. Brown, Proc. 1967 Cryogenic Engineering Conference, K.D. Timmerhaus Ed. (Plenum Press, Inc., New York, 1968).

16. J.P. Dawson and J.D. Haygwood, "Temperature Effects on the Capture Coefficient of CO_2," AEDC-TDR-251, January, 1964.

VIII. VITA

Michel Louis Chouarain was born on July 17, 1946 in Vinay (51), France. He received his primary and secondary education in Paris and Le Raincy (France). After two years of preparation at the "Lycée du Raincy" (Le Raincy, France) and the "Lycée Chaptal" (Paris, France) he entered the Advanced School of Chemistry in Lyon, France, from which he graduated in the year 1969. He has been enrolled in the Graduate School of the University of Missouri-Rolla since September, 1969, and has held a research assistantship from the Graduate Center for Cloud Physics Research during the period September, 1969, to January, 1971.